Digest Journal of Nanomaterials and Biostructures Vol. 18, No. 3, July - September 2023, p. 1139 - 1146

Preparation and characterization of germanium dioxide nanostructure for gas sensor application: effect of laser parameters

J. A. Yousif[a,b], S. Alptekin[b], A. Ramizy[a,*]
[a] *University of Anbar, College of Science, Department of Physics, Iraq*
[b] *Çankırı karatekin university, College of Science Department of Physics, Turkey*

In this article, a novel application of germanium dioxide (GeO_2) as a gas sensor is systematically reported. In detail, GeO_2 layers were deposited on quartz and n-type Si substrates, as a function of laser pulses, using combined laser ablation and thermal spray coating approaches. The attained layer/s were methodically inspected in term of their morphological, structural, and optical features; specifically, highly crystalline GeO_2 structure was obtained for samples prepared using 1500 pulses and above. In the meanwhile, the obtained particle diameters were found to be within the range of 15 to 274 nm, while the estimated optical band gaps exhibited values from 3.85 to 4.0 eV. Simultaneously, the gas sensing behavior demonstrated a well-oriented performance for all devices, however, devices treated with 2500 pulses delivered stable trend with sensitivity value as high as 3×10^{-6}. The rise/fall period revealed an adequate outcome ($\sim 10\ sec.$) for gas sensors fabricated via pulses of 1000 and above, with respected to the working temperature. The proposed framework delivers a substitute technique towards 2D metal oxide based eco-friendly-gas sensor.

(Received June 20, 2023; Accepted September 25, 2023)

Keywords: Germanium dioxide, Gas sensor, Laser ablation, Thermal spray coating

1. Introduction

Environmental pollution produced through petroleum consumption results in the need for developed toxic gases detection techniques. Such pollution causes serious damages to the surrounding environment as well as to human health. Further, gas sensors are of great interest owing to their wide-ranging applications such as medical diagnosis, agricultural production, environmental pollution monitoring, etc., through which the detection of small molecules of gas is of crucial significance [1]. Thus, a number of efforts, therefore, have been devoted for gas sensor development which operates at any pressure and/or temperature [2-5].

In this attempt, two-dimensional (2D) semiconductors within the scale of nanometer have attracted substantial consideration in the addressed field because of their substantial properties such as electron mobility, conductivity, wide energy band gap, relatively high surface to volume ratio [6-8]. Further, 2D semiconductors, such as SnO_2, ZnO, NiO, CuO, TiO_2, CdO, etc. demonstrated noteworthy performance in variety of nan-devices application; for instance, gas storage, conducting electrodes, dye-sensitized solar cells, photodetectors, and gas sensors [9-13]. As such, several efforts have been conducted to enhance/explore the utilization of 2D semiconductors for different applications; these include doping with different groups of 2D semiconductors [14-16].

A promising approach within the field of nano-devices is the utilization of novel metal oxide semiconductor materials along with exploiting their benefits in micro/nano electronics technologies for particular applications. Germanium dioxide (GeO_2) is an n-type semiconductor which has been widely investigated because of its excellent chemical and physical features, such as direct and wide energy band gap of 4.2 eV, stable structure, relatively high electron mobility, well-established air-stability and large surface area [17-19]. GeO_2 revealed an outstanding performance in variety of applications such as photodetectors, solar cells, optical modulator,

[*] Corresponding author: asmat_hadithi@uoanbar.edu.iq
https://doi.org/10.15251/DJNB.2023.183.1139

photocatalytic, lithium□storage, etc. [20-24]. Henceforth, this study reports a novel GeO_2 fabrication for gas sensor application. In detail, GeO_2 layers were fabricated using laser ablation and thermal spray coating methods. Further, the morphological, structural, optical, as well as gas sensing parameters of the attained sheets were characterized via rich tool of techniques. It was established that the obtained band gap/s behavior is directly correlated to the overall device performance.

2. Experimental work

GeO_2 layer film deposition, on both quartz and n-type Si substrates, was systematically achieved through combination of laser ablation and thermal spraying coating approaches. In a typical preparation procedure, Ge powder (Sigma Aldrich, 99.999%) was firstly mechanically pressed under 5 tons to attained a diameter of $1\,cm$ as the ablation target. Subsequently, the attained target was placed in a baker containing 3 ml deionized water (DI) where a Q-switched Nd-YAG second harmonic laser source with wavelength of 1064 nm, frequency of 10 Hz and energy of 2J was vertically positioned to ablate the fabricated target; the distance between the entrance window and the target was fixed to 12 cm. Herein, a number of pulses were utilized during the ablation process (500, 1000, 1500, 2000, and 2500). In order to ensure an evenly dispersing of the utilized nanoparticles, a continuous target rotation was maintained throughout the ablation procedure. The attained solution was stored for further use.

Continuously, the multi-cycled cleaned substrate/s using DI, ethanol, and acetone was placed on a hot plate for 10 minutes at 200 °C. Next, the spray gun was vertically position with a distance of 29 cm to the substrate; wherein the amount of the deposited solution was controlled through a built-in valve (2 ml/min) along with the applied pressure. The spray time was limited to 5 second for each layer deposition. Hereinafter, finger-shaped Al electrodes with channel height and width of 3.3 mm and 0.4 mm, respectively, were deposited via thermal evaporation technique; this in turn was accomplished under extreme vacuum using mechanical and diffusion pumps (E306A Edwards, $10^{-3} - 10^{-6}\,mbar$). The acquired samples were denoted as P-500, P-1000, P-1500, P-2000, and P-2500 in accordance with the utilized laser pulses.

The structural parameters of the coated layers were inspected using x-ray diffraction technique (Philips PW, XRD), while the morphological topographies were studied using field emission-scanning electron microscopy (S-1640 HITACHI, FE-SEM). Further, the optical properties of the fabricated layers were carried out using ultraviolet visible light spectrophotometer (DeNovix, UV-Vis). Finally, H2 gas was utilized to evaluate the fabricated gas sensor/s performance. Herein, the laboratory-based arrangement, through which the sensors' performance were evaluated, is consisted of computer-based high precision multimeter (UNI-T UT81 A) in conjunction with air-compressed vacuum chamber and gas source cylinder; the utilized gas (H2) was supplied with concentration of 150 ppm and interval period of 40 seconds.

3. Results and discussion

The XRD patterns of the thermally sprayed layers at diverse laser pulses are elucidated in Figure 1. In detail, the attained XRD curves revealed the formation of hexagonal crystalline phase of GeO_2 at around $2\theta \approx 54.6°$, 56.4°, 61.8°, and 66.7° which in turn are corresponded to the crystal planes (202), (210), (113), and (002), respectively; the obtained results are well-agreed with other reported data [24] as well as data report no. (JCSD 98-063-7456). In addition, diffraction peak obtained at around $2\theta \approx 47.8°$ is mainly due to the formation of (120) plane which corresponded to GeO_4 phase; such a singularity is mainly related to the Orthorhombic structure (COD 96-900-6860). It is worth mentioning that the GeO_4 occurred in the XRD results was only noticed after exposing the target to laser pulses above 500.

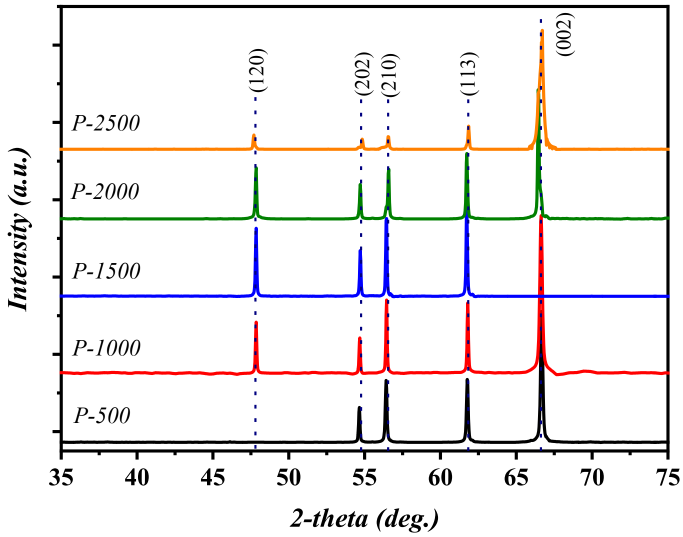

Fig. 1. XRD patterns of the deposited layers at laser pulses of 500, 1000, 1500, 2000, and 2500.

Figure 2 illustrates the optical features of the deposited layers under the effect of different laser pulses. In particular, Figure 2 (a) depicts the optical absorbance spectra wherein a clear cut-off phenomenon was perceived at around 350 nm, this in turn is mainly corresponded to the optical behavior of GeO_2. Further, a slight Hyper-chromic shift was observed at higher number of laser pulses. The optical band gap was calculated according to Tauc relation [25, 26], wherein the obtained outcomes are demonstrated in Figure 2 (b) through (f) for pulses of 500, 1000, 1500 2000, and 2500, respectively.

It can be clearly noticed that, generally, higher number of pulses resulted in lower optical band gap value. Specifically, P-500 exhibited an occurrence of optical band gap with value of 4.0 eV. This was noticeably decreased to a value of 3.9 eV under 1000 pulses. Optical band gap values of 3.9 and 3.85 eV were perceived under the effect of pulses' number of 2000 and 2500, respectively. The optical properties suggest a favorable optical band gap trend at higher number of laser pulses.

The surface morphology of the thermally sprayed layers was inspected via FE-SEM approach wherein the attained results are elucidated in Figure 3. The presented topographies revealed the occurrence of compact-irregular shape nanoparticles on the surface of the utilized substrate with particle diameter ranging from 15 nm to 274 nm. The occurred shape irregularity could be due to the effect of different number of clustering of particles; the latter could be attributed to high surface energy which in turn results in atoms agglomeration through bonds forming [27, 28]. It is worth mentioning that the average particle diameters were perceived to be 106, 140.9, 87.6, 81.68, and 117 nm for laser pulses of 500. 1000, 1500, 2000, and 2500, respectively.

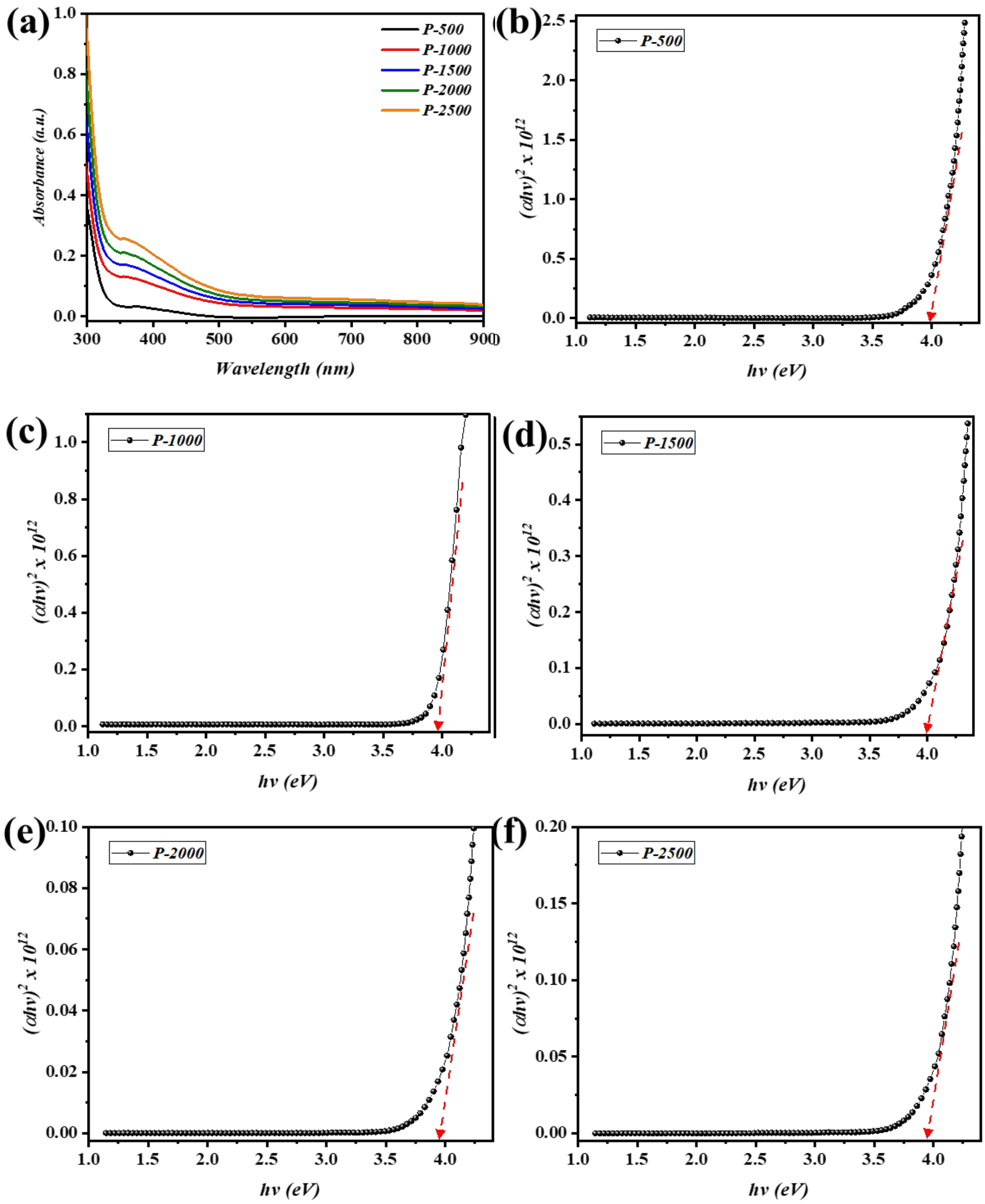

Fig. 2. (a) optical absorbance spectra, optical band gap of (b) P-500, (c) P-1000, (d) P-1500, (e) P-2000, (f) P-2500.

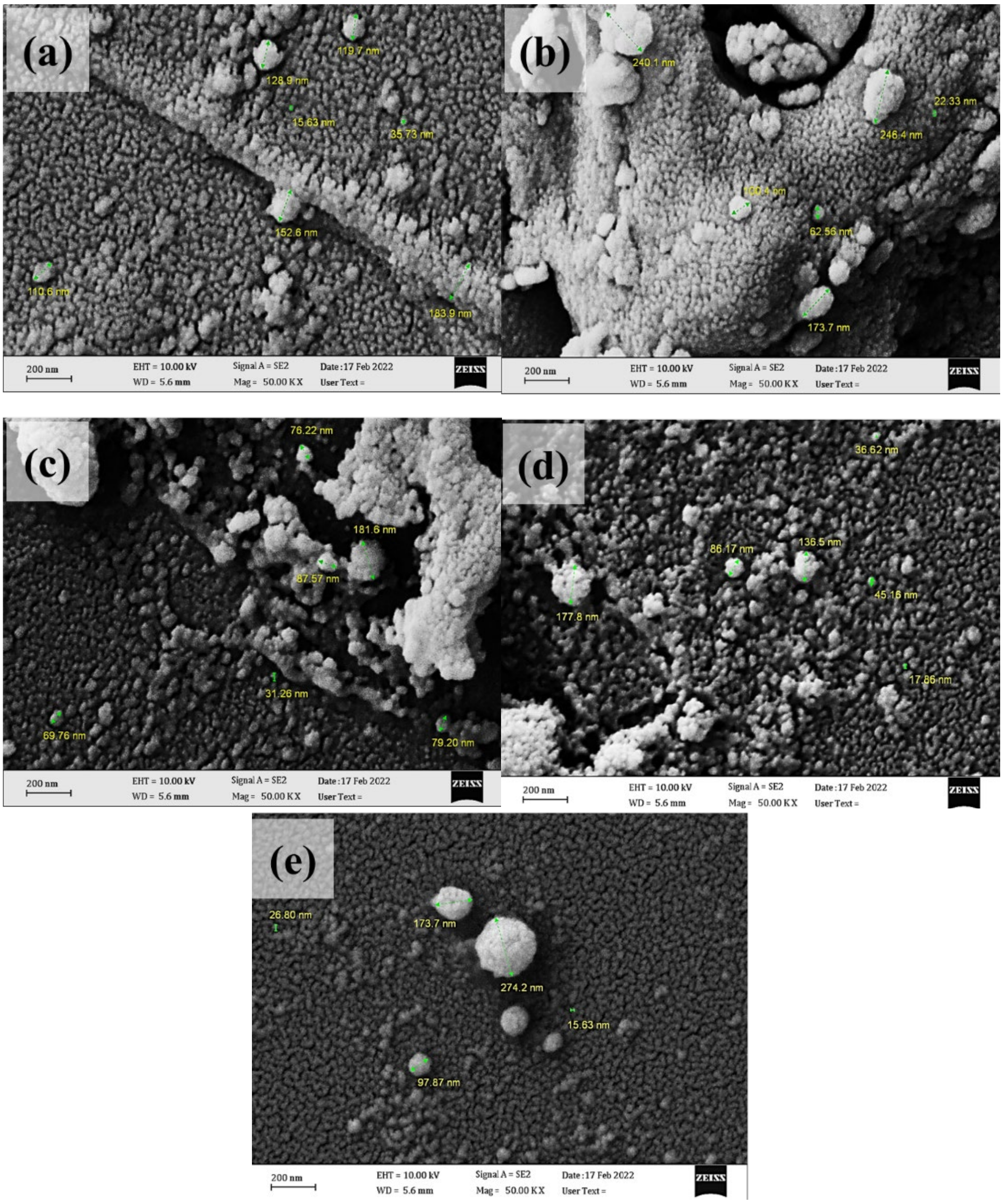

Fig. 3. FE-SEM topographies of (a) P-500, (b) P-1000, (c) P-1500, (d) P-2000, and (e) P-2500.

The switching behavior of the fabricated gas sensor as a function of the utilized laser pulses, with respect to the time intervals, is elucidated in Figure 4. The measurements were conducted under different working temperature (50 °C and 100 °C). The attained sensitivity, for all devices, increased rapidly from low to high value as the state of gas applied changed from off to on state, inset into Figure 4 (a). This could be due to the charge transfer process within the adsorbent gas and the deposited sensing layer, which in turn results in overall current increment. It is worth mentioning that the utilized semiconductor layer is n-type by which the current increment can be explain. In term of working temperature, the occurred sensitivity was observed to be linearly augmented as the temperature amplified from 50 °C to 100 °C; such observation was noticed for all fabricated gas sensors. Moreover, the behavior of the obtained sensitivity, as a function of laser pulses increment, was noticed to be similar to that acquired during the optical band gap analysis. Additionally, such a behavior could also be enlightened through the particle diameter results (Figure 3, a-e).

The response/recovery period of the fabricated gas sensors, with respect to the utilized number of pluses, was calculated from 10% to 90% of the state level (inset into Figure 4, e); the corresponded results are presented in Table 1. In general, the rise time was noticed to be higher than the fall time for all utilized laser pulses as well as the working temperature.

Table 1. Time taken for the fabricated gas sensor to rise and fall from 10% to 90% of state level.

Sample	**Temperature (°C)**	**Rise time (sec.)**	**Fall time (sec.)**
P-500	50 °C	17	5.4
P-1000		10.5	8.5
P-1500		10.5	8.3
P-2000		11	10.9
P-2500		13.5	7
P-500	100 °C	19.3	7
P-1000		10.1	8.5
P-1500		10.9	8.8
P-2000		10.9	10.7
P-2500		10.5	10

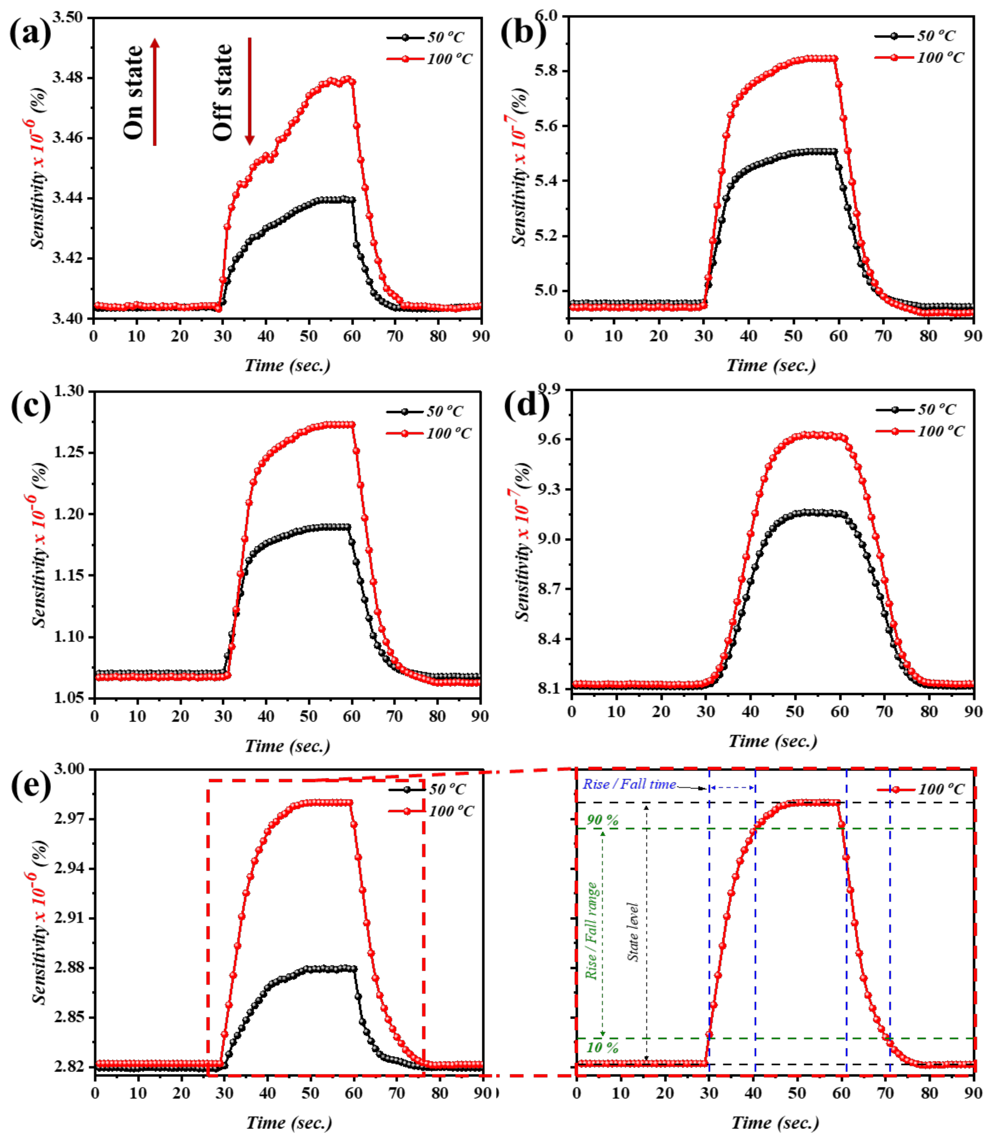

Fig. 4. Switching behavior of the fabricated gas sensors; (a) P-500, (b) P-1000, (c) P-1500, (d) P-2000, and (e) P-2500.

4. Conclusion

The fabrication of GeO_2 metal oxide via combination of laser ablation and thermal spray coating approaches for gas sensor application was reported systematically. Hereinafter, the surface, structure, and optical characteristics of the coated layers were thoroughly studied. Specifically, GeO_2 nanoparticle with highly crystalline hexagonal structure was attained using laser pulses of 1500 and above, while the prepared particle diameters were noticed to be within the range of 15 to 274 nm. The optical band gap exhibited a decreasing trend, from 4.0 eV to 3.85 eV as a function of laser pulses increment. Continuously, the fabricated gas sensor, using 2500 pulses, exhibited gas sensitivity slightly below 3×10^{-6} with response and recovery periods of ($\sim 10\ sec$). Similar switching behavior was noticed for devices attained with pulses of 1000 to 2000. However, devices fabricated using 500 laser pulses revealed noticeably higher rise time ($\sim 17 - 19.3\ sec.$) under working temperatures of 50 °C and 100 °C, respectively.

Acknowledgements

The authors would like to sincerely acknowledge the support provided by the University of Anbar which allowed the access to physics laboratory

References

[1] T. Li, W. Yin, S. Gao, Y. Sun, P. Xu, S. Wu, et al., Nanomaterials, vol. 12, p. 982, 2022; https://doi.org/10.3390/nano12060982

[2] A. S. Mohammed, O. A. Fahad, A. Ramizy, and E. Y. Salih, Ceramics International, vol. 47, pp. 17907-17914, 2021; https://doi.org/10.1016/j.ceramint.2021.03.103

[3] J. Liu, L. Zhang, J. Fan, and J. Yu, Small, vol. 18, p. 2104984, 2022; https://doi.org/10.1002/smll.202104984

[4] Q. Li, W. Zeng, and Y. Li, Sensors and Actuators B: Chemical, p. 131579, 2022; https://doi.org/10.1016/j.snb.2022.131579

[5] R. Paul, B. Das, and R. Ghosh, Journal of Alloys and Compounds, p. 168943, 2023; https://doi.org/10.1016/j.jallcom.2023.168943

[6] L. Shekari, A. Ramizy, K. Omar, H. A. Hassan, and Z. Hassan, Applied surface science, vol. 263, pp. 50-53, 2012; https://doi.org/10.1016/j.apsusc.2012.07.164

[7] M. Mahdi, A. Ramizy, Z. Hassan, S. Ng, J. Hassan, and S. Kasim, Chalcogenide Letters, vol. 9, pp. 19-25, 2012.

[8] I. M. Ibrahim, I. M. Ali, B. I. Dheeb, Q. A. Abas, A. Ramizy, M. Eisa, et al., Materials Science and Engineering: C, vol. 73, pp. 665-669, 2017; https://doi.org/10.1016/j.msec.2016.12.121

[9] E. Y. Salih, M. B. A. Bashir, A. H. Rajpar, and I. A. Badruddin, Ceramics International, vol. 48, pp. 9965-9972, 2022; https://doi.org/10.1016/j.ceramint.2021.12.203

[10] F. Salleh, R. Usop, N. S. Saugi, E. Y. Salih, M. Mohamad, H. Ikeda, et al., Applied Surface Science, vol. 497, p. 143736, 2019; https://doi.org/10.1016/j.apsusc.2019.143736

[11] M. B. A. Bashir, A. H. Rajpar, E. Y. Salih, and E. M. Ahmed, Nanomaterials, vol. 13, p. 802, 2023; https://doi.org/10.3390/nano13050802

[12] M. B. A. Bashir, E. Y. Salih, A. H. Rajpar, G. Bahmanrokh, and M. F. M. Sabri, Journal of Micromechanics and Microengineering, vol. 32, p. 085006, 2022; https://doi.org/10.1088/1361-6439/ac7d93

[13] E. Y. Salih, M. B. A. Bashir, A. H. Rajpar, I. A. Badruddin, and G. Bahmanrokh, Microelectronic Engineering, vol. 258, p. 111758, 2022; https://doi.org/10.1016/j.mee.2022.111758

[14] E. Y. Salih, A. Ramizy, O. Aldaghri, M. F. M. Sabri, N. Madkhali, T. Alinad, et al.,

Nanomaterials, vol. 12, p. 1477, 2022; https://doi.org/10.3390/nano12091477
[15] I. Ibrahim, A. Mohammed, and A. Ramizy, Journal of Ovonic Research, vol. 14, pp. 17-25, 2018.
[16] A. Obaid, M. Mahdi, A. Ramizy, and Z. Hassan, Advanced Materials Research, 2012, pp. 60-64; https://doi.org/10.4028/www.scientific.net/AMR.364.60
[17] Q.-J. Liu and Z.-T. Liu, Materials science in semiconductor processing, vol. 27, pp. 765-776, 2014; https://doi.org/10.1016/j.mssp.2014.07.047
[18] E. N. Nikolaevskaya, A. V. Kansuzyan, G. E. Filonova, V. A. Zelenova, V. M. Pechennikov, I. V. Krylova, et al., European Journal of Inorganic Chemistry, vol. 2019, pp. 676-681, 2019; https://doi.org/10.1002/ejic.201801259
[19] A. V. Kansuzyan, S. D. Farafonova, E. A. Saverina, I. V. Krylova, V. A. Balycheva, A. Y. Akyeva, et al., Mendeleev Communications, vol. 32, pp. 25-27, 2022; https://doi.org/10.1016/j.mencom.2022.01.007
[20] S. Yan, H. Song, S. Lin, H. Wu, Y. Shi, and J. Yao, Advanced Functional Materials, vol. 29, p. 1807946, 2019; https://doi.org/10.1002/adfm.201807946
[21] H. M. El-Hageen, A. M. Alatwi, and A. N. Z. Rashed, Open Engineering, vol. 10, pp. 506-511, 2020; https://doi.org/10.1515/eng-2020-0065
[22] W. J. Kim, V. Soshnikova, J. Markus, K. H. Oh, G. Anandapadmanaban, R. Mathiyalagan, et al., Optik, vol. 178, pp. 664-668, 2019; https://doi.org/10.1016/j.ijleo.2018.09.182
[23] T. A. Amollo, G. T. Mola, and V. O. Nyamori, Materials Chemistry and Physics, vol. 254, p. 123448, 2020; https://doi.org/10.1016/j.matchemphys.2020.123448
[24] S. O. Abdulghani, E. Y. Salih, and A. S. Mohammed, Materials Chemistry and Physics, p. 127859, 2023; https://doi.org/10.1016/j.matchemphys.2023.127859
[25] M. B. A. Bashir, E. Y. Salih, M. F. M. Sabri, A. H. Rajpar, I. A. Badruddin, M. Z. Hussein, et al., ECS Journal of Solid State Science and Technology, vol. 10, p. 106006, 2021; https://doi.org/10.1149/2162-8777/ac2b3b
[26] E. Y. Salih, A. Ramizy, O. Aldaghri, M. F. Mohd Sabri, N. Madkhali, T. Alinad, et al., Crystals, vol. 12, p. 79, 2022; https://doi.org/10.3390/cryst12010079
[27] N. Bose, M. Basu, and S. Mukherjee, Materials Research Bulletin, vol. 47, pp. 1368-1373, 2012; https://doi.org/10.1016/j.materresbull.2012.03.009
[28] E. Gorokhov, K. Astankova, A. Komonov, and A. Kuznetsov, Laser Pulses− Theory, Technology, and Applications, INTECH, Rijeka, pp. 383-436, 2012; https://doi.org/10.5772/53481